

Comparison of Electrode Reduction Activities of *Geobacter sulfurreducens* and an Enriched Consortium in an Air-Cathode Microbial Fuel Cell^{∇†}

Shun'ichi Ishii,^{1,4*} Kazuya Watanabe,^{2,5} Soichi Yabuki,¹ Bruce E. Logan,³ and Yuji Sekiguchi¹

Institute for Biological Resource and Functions, National Institute of Advanced Industrial Science and Technology (AIST), 1-1-1 Higashi, Tsukuba, Ibaraki 305-8566, Japan¹; Research Center for Advanced Science and Technology, University of Tokyo, 4-6-1 Komaba, Tokyo 153-8904, Japan²; Department of Civil and Environmental Engineering, Penn State University, University Park, Pennsylvania 16802³; JSPS, 1-6 Chiyoda-ku, Tokyo 102-8471, Japan⁴; and Hashimoto Light Energy Conversion Project, ERATO, JST, Hongo, Bunkyo-ku, Tokyo 113-8656, Japan⁵

Received 16 July 2008/Accepted 29 September 2008

An electricity-generating bacterium, *Geobacter sulfurreducens* PCA, was inoculated into a single-chamber, air-cathode microbial fuel cell (MFC) in order to determine the maximum electron transfer rate from bacteria to the anode. To create anodic reaction-limiting conditions, where electron transfer from bacteria to the anode is the rate-limiting step, anodes with electrogenic biofilms were reduced in size and tests were conducted using anodes of six different sizes. The smallest anode (7 cm², or 1.5 times larger than the cathode) achieved an anodic reaction-limiting condition as a result of a limited mass of bacteria on the electrode. Under these conditions, the limiting current density reached a maximum of 1,530 mA/m², and power density reached a maximum of 461 mW/m². Per-biomass efficiency of the electron transfer rate was constant at 32 fmol cell⁻¹ day⁻¹ (178 μmol g of protein⁻¹ min⁻¹), a rate comparable to that with solid iron as the electron acceptor but lower than rates achieved with fumarate or soluble iron. In comparison, an enriched electricity-generating consortium reached 374 μmol g of protein⁻¹ min⁻¹ under the same conditions, suggesting that the consortium had a much greater capacity for electrode reduction. These results demonstrate that per-biomass electrode reduction rates (calculated by current density and biomass density on the anode) can be used to help make better comparisons of electrogenic activity in MFCs.

Microbial fuel cells (MFCs) are devices that exploit microorganisms as “biocatalysts” of generating electric power from organic matter. MFC systems are being researched as a method of recovering energy from waste as electrical power (10, 23, 24, 35) and generating power from aquatic sediments on the bottom of the ocean (25, 42) or from rice paddy soil (13, 14). Recent technical improvements of MFC system architecture have increased power densities from <0.1 mW/m² to >2,400 mW/m² (normalized by the anode surface area) during the past several years in systems lacking exogenous electron shuttles (22, 24). However, continued improvements are still needed for improved power densities, reduced costs for materials, and the development of large-scale devices (8).

The two common ways of expressing MFC performance for power generation are power normalized to the projected surface area of an electrode (power density; mW/m²) and power per unit of reactor volume (power output; W/m³) (35). Many studies of MFCs have used power density based on the assumption that the biocatalytic activity of the anode limits power production (16, 24, 35, 39). However, variations in the reactor volume (2, 38), composition of the proton-exchange membrane (17), catholyte reactions (32, 34), substrates (21), and anode materials (5, 33) often make it difficult to know

which factors actually limit power production. There are various potential losses that can limit power output, such as microbial electron transfer to the anode, solution resistance, membrane resistance, and reduction reaction on the cathode (16, 35). These can be classified into the following three major rate-limiting processes: (i) the anodic reaction limited by microbial activity, (ii) the cathodic reaction limited by the abiotic electron-accepting reaction, and (iii) other abiotic factors, including diffusion of substrate to the microbes, oxygen diffusion, and proton transfer through the membrane (16, 35). To better understand and improve power generation of MFCs, factors affecting each of these limiting steps need to be carefully and separately examined.

Mediatorless MFCs typically operate at electrical current densities of 0.1 to 2 mA/cm², which are lower by two orders of magnitude or more than those achieved in enzyme-based biofuel cells or hydrogen fuel cells (1, 9, 33). While current production by the bacteria can be one of the reasons for lower current densities, the relationship between bacterial colonization of the anode and current generation has not been directly shown, and the amount of biomass per surface area of the anode has not been conclusively linked to power production. We therefore investigated current generation and biomass density in an MFC under anodic reaction-limiting conditions by reducing the anode size (and therefore the total surface area) in a single-chamber, air-cathode MFC using both a pure culture and a consortium. In an air-cathode MFC, the cathode is directly exposed to air on one side and liquid on the other. In contrast, an aqueous cathode is submerged in fluid, and if oxygen is used as the electron acceptor, the cathode solution must be aerated (6). MFCs with air cathodes produce higher

* Corresponding author. Mailing address: National Institute of Advanced Industrial Science and Technology (AIST), 1-1-1 Higashi, Tsukuba, Ibaraki 305-8566, Japan. Phone: 81-29-861-6026. Fax: 81-29-861-6400. E-mail: shunichi-ishii@aist.go.jp.

† Supplemental material for this article may be found at <http://aem.asm.org/>.

∇ Published ahead of print on 3 October 2008.

power densities than aqueous cathodes due to the more efficient oxygen and proton transfer to the electrode (20). We examined power generation using the air-cathode MFC, as this type of reactor is the most likely system to be used in practical applications such as wastewater treatment (10, 23). The system used here has previously been demonstrated to produce up to 600 mW/m² per cathode surface area and 130 mW/m² per anode surface area with mixed cultures in 200 mM phosphate-buffered saline medium with a flat anode (22). However, maximum power densities are known to be affected by solution conductivity, electrode sizes, and other factors, and therefore, the maximum power density cannot be predicted from a past experiment if reactor conditions are changed (17, 21, 22, 32).

Geobacter sulfurreducens PCA, a well-studied, electricity-generating (exoelectrogenic) bacterium, was chosen as a model microorganism in order to relate current production to biocatalytic activity normalized by bacterial cell numbers (3, 41). Strain PCA grows using acetate or hydrogen as an electron donor and ferric pyrophosphate (Fe-PP_i), ferric oxyhydrate [amorphous Fe(III) oxide], ferric citrate, elemental sulfur, or fumarate as the sole electron acceptor (4). Power production by *G. sulfurreducens* was recently found to be comparable to that produced by a mixed culture in an MFC using a ferricyanide catholyte (31). However, power production was not examined on the basis of biomass per area. By measuring biomass on the MFC anode, we were able to compare electrode reduction rates between the *Geobacter sulfurreducens* strain PCA and a consortium enriched on acetate under anodic reaction-limiting conditions on a per-biomass basis. We also compared respiration rates of the strain PCA obtained from current densities with those obtained using fumarate, soluble iron, and insoluble iron as electron acceptors on a per-cell basis.

MATERIALS AND METHODS

Microorganisms and culture conditions. *Geobacter sulfurreducens* PCA (DSM 12127) was obtained from Deutsche Sammlung von Mikroorganismen und Zellkulturen GmbH (Brunswick, Germany). The basal medium used for cultivation of the microorganism contained (per liter) the following: 0.1 g KCl, 1.5 g NH₄Cl, 0.6 g NaH₂PO₄, 0.03 g MgSO₄ · 7H₂O, 0.01 g CaCl₂ · 2H₂O, 2.0 g NaHCO₃, 0.5 g L-cysteine, 10 ml vitamin solution (12), 1 ml Se/W solution (12), and 10 ml trace mineral element solution (12). Cultivation was conducted using a 5-ml inoculum in static bottles (125 ml in capacity, sealed with a Teflon-coated butyl rubber septum and secured with a crimped aluminum cap) containing 50 ml of the medium supplemented with 10 mM acetate and 40 mM fumarate at 37°C under an N₂/CO₂ (80/20 [vol/vol]) atmosphere, without shaking. Poorly crystalline Fe(III) oxide was synthesized by neutralizing a solution of 0.4 M FeCl₃ as previously described (27). For Fe(III) oxide reduction, 38 mM of Fe(III) oxide and 10 mM of acetate were added to the basal medium. Conductivity of the basal medium (omitting L-cysteine for MFC operation) was 6.8 mS/cm, measured by using a conductive meter (Horiba, Japan).

MFC configuration and operation. A single-chamber, air-cathode MFC was used to examine power generation by both the *G. sulfurreducens* strain PCA and a consortium. The MFC was a bottle-type reactor (350 ml in capacity) equipped with a single-side port containing the air cathode as previously reported (22). The top of the bottle was sealed using a tight butyl-rubber stopper pierced with two nickel wires. Two anode electrodes made of carbon cloth (9 cm by 3 cm, or 54 cm² of total projected surface area per electrode; TML, Japan) were connected to the nickel wires and placed parallel to each other in the bottle (108 cm² of initial anode surface area). The distance from the anodes to the cathode was carefully adjusted to be the same for both anodes. The air cathode was made by coating platinum (0.5 mg/cm²) to the water-facing side using Nafion as a binder and four diffusion layers of polytetrafluoroethylene on a 30 wt% wet-proofed carbon cloth (type B-1B; E-TEK) as described elsewhere (6). The air cathode

was placed at the end of the side port, providing a total projected cathode surface area (on one side) of 4.9 cm² (22).

After sterilization of the fully assembled MFC, the chamber was anaerobically filled in a glove box (an N₂/H₂/CO₂ ratio of 80/10/10 [vol/vol/vol]) with 320 ml of the sterilized anaerobic basal medium (omitting L-cysteine) supplemented with 20 mM acetate as an electron donor and 40 mM fumarate as an electron acceptor for preliminary bacterial growth in the chamber. The chamber was inoculated with a 30-ml suspension of the strain PCA, gently mixed with a magnetic stirrer, and then incubated outside the glove box at 37°C under open-circuit conditions. The electrodes were connected with an external resistor (510 Ω) 2 days after inoculation. Cell voltages across the resistor were recorded every 30 min using a recorder (VR-71; T and D, Japan). When the electric current decreased due to depletion of acetate, additional substrate was added into the medium, and the medium was fully replaced with the fresh medium supplemented with 20 mM acetate in the glove box. To obtain polarization and power density curves, the enriched anode was placed in an otherwise identical MFC equipped with an Ag/AgCl reference electrode (+200 mV versus standard hydrogen electrode [SHE], RE-1B; ALS Co., Ltd.). The external resistance was then changed stepwise from 3.3 kΩ to 10 Ω (3.3 kΩ, 1.5 kΩ, 750 Ω, 300 Ω, 100 Ω, 51 Ω, and 10 Ω), and the cell voltage, the anode potential, and the cathode potential were recorded after they had stabilized over a period of at least 7 min (45). In order to make anodic reaction-limiting conditions with decreased anode surface areas, the anode was cut to reduce its size using ethanol-sterilized scissors in a glove box, and the polarization and power density curves were again determined as described above.

MFC operation of a consortium. An electricity-generating consortium was enriched in the same MFC using sludge (100 ml) from an anaerobic digester decomposing sewage sludge in Niigata, Japan. The chamber was filled with 250 ml of sterilized anaerobic basal medium (omitting L-cysteine) supplemented with 20 mM acetate as an electron donor and two carbon cloth anodes (6 cm by 3 cm, or 72 cm² total projected surface area). After inoculation at an external resistance of 510 Ω, the medium was replaced on days 6 and 9. On day 28, the enriched anode was placed in another MFC equipped with an Ag/AgCl reference electrode and containing fresh medium (20 mM acetate) in a glove box. Various polarization curves were determined as described above.

PCR amplification, cloning, and sequencing of 16S rRNA gene fragments. Total DNA was extracted from biofilms on the carbon cloth of the anode using a FastDNA spin kit for soil (Qbiogene) according to the manufacturer's instructions. PCR amplification of 16S rRNA gene fragments was performed using U530f (5'-GTGNCAGCMGCGCGG-3') (18) as a forward primer and U1492r (5'-GGNTACCTTGTTACG-3') (19) as a reverse primer. The PCR solution (50 μl) contained 1.25 U of *Taq* DNA polymerase (ExTaq; Takara), 10 mM Tris-HCl (pH 8.3), 50 mM KCl, 1.5 mM MgCl₂, 0.001% (wt/vol) gelatin, deoxynucleoside triphosphate at a concentration of 200 μM each, 50 pmol of each primer, and an appropriate amount of template DNA. The amplification conditions were as follows: an initial step of 95°C for 10 min; 25 cycles consisting of 95°C for 1 min, 50°C for 1 min, and 72°C for 2 min; and a final elongation step at 72°C for 10 min. The PCR cycles were set at minimum values at which sufficient quantities of products were obtained. Amplified fragments were purified with a QIAquick PCR purification kit (Qiagen), ligated into the pGEM-T vector (Promega), and cloned into *Escherichia coli* competent cells as previously described (13). *E. coli* colonies harboring clones were selected on Luria-Bertani plates supplemented with ampicillin (50 μg ml⁻¹). PCR-amplified 16S rRNA gene fragments were recovered from colonies by PCR analysis using primers T7W (5'-TAATACGA CTCATATAGGGC-3') and SP6W (5'-ATTTAGGTGACACTATAGAATA CTC-3') (the primers targeted the pGEM-T vector sequences flanking the insertion) as described previously (13). Clones containing appropriate sizes of the insertion were selected by electrophoresis analysis, and their partial nucleotide sequences were directly determined on a Beckman CEQ8000 DNA sequencer using a CEQTM DTCS Quick Start kit (Beckman Coulter) using primer U907r (5'-CCGYCAATTCMTTTRAGTTT-3') (46).

Phylogenetic analyses. Sequences of partial 16S rRNA genes determined in this study were aligned to each other using ClustalW version 1.7 (44) and assigned to phylotypes (classified as a unique clone). Database searches for related 16S rRNA gene sequences were conducted using the BLAST program (15) and the GenBank nucleotide sequence database. Checks for chimeric sequences were conducted using the Chimera Check program in the Ribosomal Database Project database (29).

Calculations. Current density was calculated from the voltage measured across the resistor as $i = I/A_{An} = V/RA_{An}$, where i (mA/m²) is the current density per anode surface area, V (mV) is the cell voltage, I (mA) is the current, R (Ω) is the external resistance, and A_{An} (m²) is the total projected anode surface area, respectively. Power density was calculated as P_{anode} (mW/m²) = $(IV \times 10^{-3})$

A_{An} , and power output was calculated as $P_{reactor} (W/m^3) = (IV)/L$, where L (ml) is the reactor volume. Coulombic efficiency, C_E (%), was calculated as $C_E = C_p/C_{th} \times 100$, where C_p (C) is the total charge passed during the experiment and C_{th} (C) is the theoretical amount of charge estimated from the consumption of acetate (eight electrons per acetate). The electron flow rate (moles of electrons/second) was calculated from the current using Faraday's constant (96,500 C/mol).

Chemical analyses. Acetate and other volatile fatty acids were determined using a high-pressure liquid chromatograph (organic acid analysis system; Shimadzu) equipped with a conductivity detector (CDD-10Avp; Shimadzu) and dual-packed columns (Shim-pack SCR-H; Shimadzu). The eluant was a mixture (equal volumes) of 5 mM *p*-toluenesulfonic acid solution and 20 mM Bis-Tris solution containing 5 mM *p*-toluenesulfonic acid and 100 μ M EDTA at a flow rate of 0.8 ml/min. Fe(II) that was soluble after a 1-h extraction with 0.5 N HCl was determined with ferrozine as described previously (26).

In order to determine the total bacterial cell density on the anode surface, protein was extracted from the electrodes as described previously (3). Part of the anode (1 cm by 1 cm) containing cells was removed from the MFC ($n = 3$). This piece of the electrode was placed in a test tube with 2 ml of 0.2 N NaOH at 4°C for 1 h and vortexed every 15 min for 10 s. The extracted liquid was pooled, and the electrode was further rinsed with 2 ml of deionized water. The liquids were mixed together (a final concentration of 0.1 N NaOH), frozen at -20°C, and thawed at 90°C for 10 min. This freeze-thaw cycle was conducted three times. Whole protein was measured by the bicinchoninic acid method against a bovine serum albumin standard in 0.1 N NaOH (Pierce). Planktonic biomass in the culture broth was measured by a similar method after planktonic cells were harvested by centrifugation at $13,000 \times g$ for 10 min. In order to correlate bacterial cell concentrations to whole protein, direct counts were performed using *Geobacter sulfurreducens* cells grown with either fumarate or Fe(III) oxide as an electron acceptor. The cells were stained with 2 mg/liter of 4,6-diamidino-2-phenylindole (DAPI) for 5 min. The DAPI-stained cells were collected on an Isopore membrane (0.22- μ m-pore diameter; Millipore Corp.) and counted using an AX80 fluorescence microscope (Olympus).

SEM. Scanning electron microscopy (SEM) observation was performed as described previously (11). A small portion of carbon cloth containing cells was carefully removed from the anode in an anaerobic glove box, and the cells were fixed with 1.25% glutaraldehyde and 1.3% osmium tetroxide. After cells were dehydrated using a graded series of ethanol solutions, they were dried using an HCP-2 drier (Hitachi). The resultant specimen was coated with osmium for 5 s using a coating device (Neoc-ST; Meiwafoosis) and observed using a scanning electron microscope (S4500; Hitachi) at 10 kV. Fresh carbon cloth (no pretreatment) was similarly observed.

Nucleotide sequence accession numbers. The nucleotide sequences reported in this paper have been deposited in the GSDB, DDBJ, EMBL, and NCBI nucleotide sequence databases under accession numbers AB447522 to AB447535.

RESULTS

Power generation in an air-cathode MFC. Following 2 days of growth of *G. sulfurreducens* PCA cells under open-circuit conditions in an air-cathode MFC, current was immediately generated when the circuit was closed (510 Ω of external resistance) and the reactor was switched to MFC operation (see Fig. S1A in the supplemental material). There was no current generated by an abiotic control (data not shown). The voltage increased for 3 days and then stabilized at approximately 360 mV (0.72 mA). This voltage was stable for over 2 weeks, independent of continued bacterial growth in the MFC. When the voltage rapidly decreased due to acetate depletion, 10 mM acetate was added as the electron donor, resulting in rapid recovery to the same output voltage. Following a decrease in cell voltage, the solution was completely replaced with fresh medium (20 mM acetate) to omit planktonic cells and any possible soluble compounds functioning as electron shuttles. Identical voltages and currents were again achieved, indicating that stable power production was not affected by planktonic

cells or by the presence of soluble compounds that might function as mediators, consistent with previous reports (3, 30).

When stable power output was observed, the external resistor was changed from 510 Ω to 10 Ω (see Fig. S1B in the supplemental material). The cell voltage quickly decreased to 25 mV ($I = 2.5$ mA), and the power output was stable for over 3 days. When the external resistor was changed back from 10 Ω to 510 Ω , however, the cell voltage increased slowly until it reached 340 mV ($I = 0.68$ mA). This result indicated that the *Geobacter sulfurreducens* cells needed at least 2 h to acclimatize to a change from a low to a high external resistance. Thus, a gradual decrease in external resistance is better for developing a polarization curve than a rapid increase in resistance. The coulombic efficiency was 52% (0.42 mmol liter⁻¹ day⁻¹ of acetate; 0.68 mA) at 510 Ω , and it increased to 79% at 10 Ω due to an increase in acetate utilization and current (1.03 mmol liter⁻¹ day⁻¹ of acetate; 2.5 mA) (duplicate reactors). These results are consistent with previous reports using mixed cultures that show a trend of increased coulombic efficiency with current production (7, 21, 22).

Limiting current density under anodic reaction-limiting conditions. Six polarization curves were obtained using different anode surface areas (68 cm², 54 cm², 36 cm², 27 cm², 14 cm², and 7 cm²) after the anode was placed in a new MFC on day 216 (Fig. 1). Two different trends were observed for these polarization curves. Using larger anodes (from 27 cm² to 68 cm²), cell voltage proportionally decreased with current due to ohmic polarization of the cathode potential (Fig. 1A), suggesting ohmic potential losses were dominated by internal resistance. For these conditions, maximum power generation was limited by cathode polarization (ohmic loss-defined condition). For smaller anodes, the cell voltage rapidly decreased at a specific current (2.1 mA at 14 cm² and 0.9 mA at 7 cm²) (Fig. 1A). These sharp decreases in cell voltage were likely caused by the potential loss of the anode at the specific current (Fig. 1A), indicating that an anodic reaction-limiting condition was produced when using small anodes (7 cm² or 14 cm²). Under this anodic reaction-limiting condition, the current density per anode surface area was much higher than that obtained under ohmic loss-defined conditions (although the maximum current was less than that produced with a larger anode) (Fig. 1B).

Analysis of the peak current densities (all at 10 Ω) shows that current density versus anode surface area clearly showed the potential limiting current density (1,530 mA/m²) at anode surface areas smaller than 14 cm² (Fig. 2A). Thus, there were anodic reaction-limiting conditions when anodes smaller than 14 cm² were used. Under these anode-limited conditions, the bacteria functioned more effectively to transfer electrons from cells to the anode. Consequently, for anodic reaction-limiting conditions, the catalytic activity of the *Geobacter sulfurreducens* cells adhered on the anode-limited current density to 1,530 mA/m². Power density continued to increase with a decrease in the anode surface area. The maximum value of power density found for the smallest anode was 461 mW/m² (300 Ω ; $A_{An} = 7$ cm²) (Fig. 2B).

Biomass density versus limiting current density. The electrolyte was replaced with fresh medium on days 66, 133, 148, 172, and 216, allowing bacterial growth to continue on the anode but not in the suspension. SEM images of the anode on day 11 revealed that the biofilm was very nonhomogeneous at

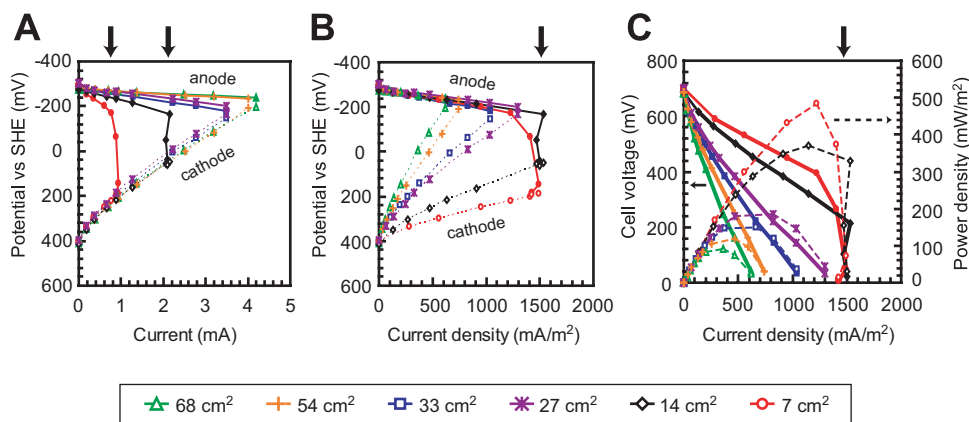


FIG. 1. Polarization and power curves for various anode surface areas in an air-cathode MFC with *Geobacter sulfurreducens* cells on day 216. Anode potential (thin lines in panels A and B), cathode potential (broken lines in panels A and B), and cell voltages (thick lines in panel C) were measured at various external resistances and plotted versus electrical current (A) or current density normalized to the projected anode surface area (B and C). Reactor performance of the MFC was represented by power density per anode surface area (broken line in panel C). Arrows indicate anodic reaction-limiting conditions.

the microscopic level (Fig. 3B), although the biomass density on the electrode appeared homogeneous at the macroscopic level for the *Geobacter* biofilms. There were many large aggregates observed on the carbon cloth, and the electrode was partially covered by the bacterial cells. After long-term operation (over 216 days), the coverage of *Geobacter sulfurreducens* cells on the surface increased, resulting in a dense biofilm on the anode (Fig. 3C). The biomass density on the electrode was $1.35 \times 10^9 \pm 0.06 \times 10^9$ cells/cm² (0.18 mg of protein/cm²; 19.8 mg of total protein on the anode) on day 11 and was $2.82 \times 10^9 \pm 0.42 \times 10^9$ cells/cm² (0.39 mg of protein/cm²; 31.3 mg of total protein on the anode) on day 68, respectively. On day 68, before the solution was removed, the mass of planktonic cells was measured as 4.2 mg, indicating 92% of the biomass in the MFC was on the anode. On day 216, the biomass density on the electrode increased slightly to $3.91 \times 10^9 \pm 0.32 \times 10^9$ cells/cm² (0.53 mg of protein/cm²; 43.3 mg of total protein). Calculations were subsequently based only on cells adhering to the anode.

The limiting current densities on days 11 and 68 were also determined under anodic reaction-limiting conditions by creating smaller anode surface areas (data not shown). The limiting current density increased during the MFC operation, with 482 mA/m² on day 11 ($A_{An} = 27$ cm²), 963 mA/m² on day 68 ($A_{An} = 14$ cm²), and 1,530 mA/m² on day 216 ($A_{An} = 7$ cm²). These results indicated that the limiting current density changed in proportion to biomass densities on the anode (Fig. 4). This relationship between cell adhesion and limiting current density suggested that the per-cell electron transfer rate was constant under anodic reaction-limiting conditions, indicating that the potential per-cell electrode reduction rate was independent of the growth phase and biofilm thickness of *G. sulfurreducens* PCA during MFC operation.

Electrode reduction rate of *Geobacter sulfurreducens* cells. In order to analyze per-biomass efficiency of current production, we examined the microbial potential activity of electron flow rate normalized to a single bacterial cell on the MFC anode. Based on measured biomass densities correlated with the limiting current densities, per-biomass electron transfer rate to

the anode was calculated as the electrode reduction rate. The per-biomass electron donation rate onto the anode was 32 ± 2 fmol cell⁻¹ day⁻¹ ($178 \mu\text{mol g of protein}^{-1} \text{min}^{-1}$) for *G. sulfurreducens* PCA. In order to compare these results to rates obtained with other electron acceptors, we measured fumarate and Fe(III) oxide reduction rates for cells growing exponentially (data not shown). The reduction rates for cells were 23 ± 8 fmol cell⁻¹ day⁻¹ for solid iron and 103 ± 6 fmol cell⁻¹ day⁻¹ for fumarate, respectively. The rate for cells using Fe(III) PP_i is 225 ± 33 fmol cell⁻¹ day⁻¹, reported previously (4). The electron donation rate onto the anode was most similar to that of solid iron reduction, with much-higher rates obtained for soluble electron acceptors (fumarate and soluble iron). These results suggest that the electron transfer rate to the anode is constrained in a manner similar to that of solid iron reduction, consistent with previous reports (3, 37).

Electrode reduction rate of an enriched consortium. Electrode reduction rates can vary with the type of MFC, solution conditions, and relative sizes of the electrodes, and many experiments have been conducted only with a consortium. In order to provide a basis for comparison of results obtained here with *G. sulfurreducens* PCA regarding how this system might perform with a mixed consortium, we enriched a MFC with a consortium in the same acetate medium. The current generated with this inoculum stabilized at ~ 0.76 mA within 3 weeks (see Fig. S2 in the supplemental material). The coulombic efficiency was 19% ($1.54 \text{ mmol liter}^{-1} \text{day}^{-1}$ of acetate; 0.88 mA) at 510 Ω and increased to 41% at 10 Ω due to an increase in acetate utilization and current ($2.92 \text{ mmol liter}^{-1} \text{day}^{-1}$ of acetate; 3.7 mA), respectively. This low coulombic efficiency was likely caused by substrate consumption by methanogens and/or heterotrophic growth of bacteria using oxygen that diffused through the air cathode (6, 13, 20).

In order to determine limiting current density under anodic reaction-limiting conditions, polarization curves were obtained using four different anode surface areas (72 cm², 50 cm², 36 cm², and 11 cm²) (see Fig. S3 in the supplemental material). At an anode surface area of 11 cm², cell voltages sharply decreased to ~ 1.3 mA, indicating the anodic reaction-limiting

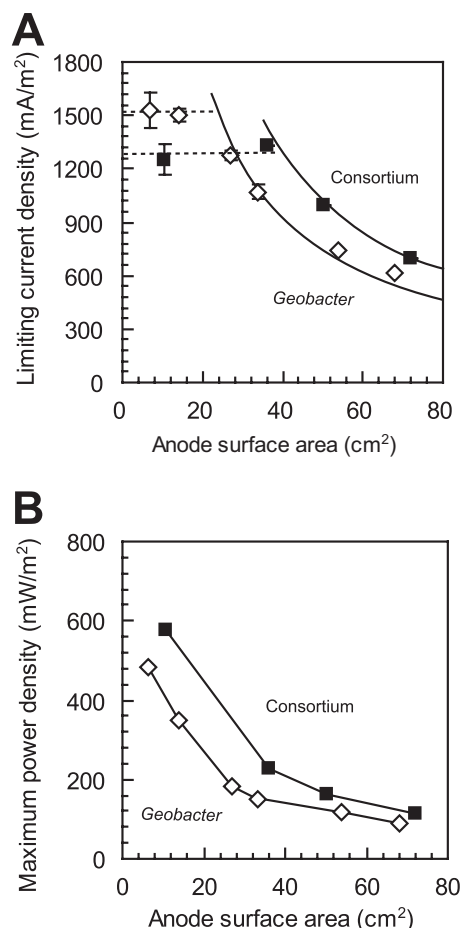


FIG. 2. (A) Limiting current density of the strain PCA (open diamond) and the enriched consortium (solid square) generated with 10 Ω of external resistor correlated with projected anode surface areas (on day 216 of the strain PCA and day 28 of the consortium). The curved lines show that there are inverse relationships between current density and anode surface area under ohmic loss-defined conditions when maximum currents are constant (3.7 mA of the *G. sulfurreducens* strain PCA and 5.0 mA of the consortium). The dashed lines show that limiting current densities reach 1,530 mA/m² of the *G. sulfurreducens* strain PCA or 1,250 mA/m² of the consortium when the anode surface area is less than 14 cm² (PCA) or less than 36 cm² (consortium). (B) Maximum power density of the *G. sulfurreducens* strain PCA and the consortium generated correlated with projected anode surface areas (on day 216 of the strain PCA and day 28 of the consortium).

condition at this surface area. The limiting current density was 1,250 mA/m², and the maximum power density for the smallest anode (11 cm²) was 576 mW/m² (Fig. 2). The electrolyte was fully replaced with fresh medium before obtaining the polarization curves to ensure that current generation was independent of planktonic cells and any self-produced electron shuttles.

The biomass density on the anode on day 28 was 208 ± 20 μ g of protein/cm², which is similar to that of the *Geobacter sulfurreducens* biofilm on day 11. The biofilm of the anode consortium on day 28 similarly revealed heterogeneous coverage and the appearance of large aggregates similar to those of the *Geobacter sulfurreducens* biofilm on day 11 (Fig. 3D). A per-biomass electrode reduction rate for the consortium MFC

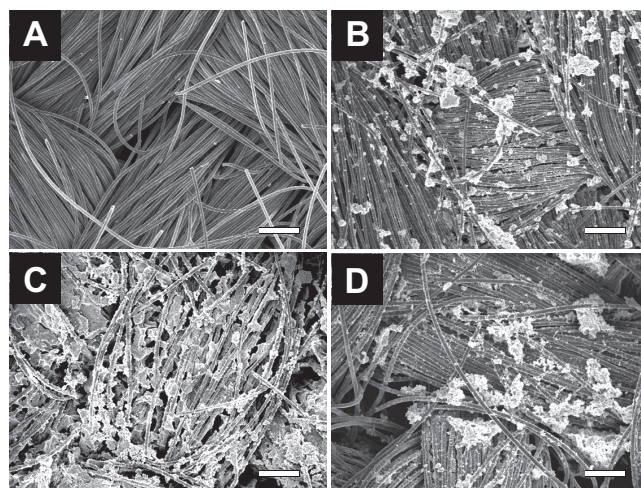


FIG. 3. SEM images of the original carbon cloth for the anode (A), a biofilm of *Geobacter sulfurreducens* cells onto the anode on day 11 (B) and day 216 (C), and a consortium biofilm on the anode on day 28 (D). Bars, 100 μ m.

was calculated to 373 μ mol g of protein⁻¹ min⁻¹ under anodic reaction-limiting conditions. This result suggests that the biocatalytic capacity of electron transfer to the anode of the consortium is approximately two times higher than that of *G. sulfurreducens* PCA. The reasons for this higher rate by the mixed culture are not known.

Phylogenetic composition. In order to identify which organisms were present in these biofilms, we constructed 16S rRNA gene clone libraries of the enriched consortium. To obviate biases associated with PCR amplification as much as possible, we selected a universal PCR primer set and minimized PCR cycles. Results of the clone library analysis are summarized with phylogenetic affiliations in Table 1. It is shown that half of the clones were affiliated with the phylum *Proteobacteria*, while others were affiliated with *Firmicutes* and *Bacteroidetes*. The result indicates that almost all of the cells on the anode are anaerobic bacteria. The major phylotypes (those including more than three clones) were two *Deltaproteobacteria* isolates (N1-22 and N1-2) and one *Bacteroidetes* isolate (N1-25). Phylotypes N1-22 and N1-2 are closely correlated with *Geobacter sulfurreducens* PCA. The phylotypes may also have represented

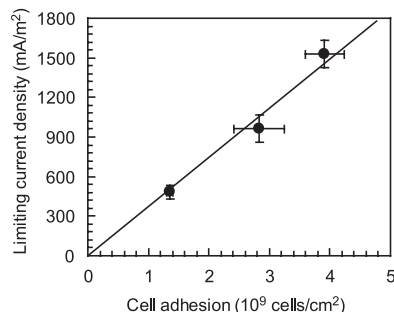


FIG. 4. Proportional relationship between biomass density on the anode and limiting current density for an anodic reaction-limiting condition on the *Geobacter sulfurreducens* MFC. The values were determined on days 11, 68, and 216 ($n > 3$).

TABLE 1. Phylotypes obtained from the enriched electricity-generating consortium

Phylotype	No. of clones in the library (total = 24)	% Database match (accession no.)
<i>Proteobacteria</i>		
N1-22	4	98% <i>Geobacter sulfurreducens</i> (U13928)
N1-2	3	99% <i>Geobacter sulfurreducens</i> (U13928)
N1-5	1	96% <i>Azonexus</i> sp. strain RV3 (DQ833391)
N1-7	1	99% <i>Comamonas denitrificans</i> (DQ836252)
N1-21	1	98% <i>Alcaligenes</i> sp. strain B89Ydz-zz (EU070357)
N1-30	1	97% <i>Geobacter sulfurreducens</i> (U13928)
<i>Firmicutes</i>		
N1-13	2	97% <i>Sedimentibacter</i> sp. strain JN18_A14_H (DQ168650)
N1-1	1	93% <i>Clostridiales</i> bacterium JN18_A24_M (DQ168655)
N1-4	1	86% <i>Clostridium cochlearium</i> (M59093)
N1-19	1	87% <i>Eubacterium</i> sp. strain Pei061(AJ629069)
N1-23	1	97% " <i>Frigovirgula patagoniensis</i> " (AF450134)
<i>Bacteroidetes</i>		
N1-25	3	99% Uncultured bacterium B1C2-8 (EU481656)
N1-3	2	92% <i>Paludibacter propionicigenes</i> (AB078842)
Unknown		
N1-20	2	90% Uncultured bacterium W18 (DQ238245)

important populations to generate electricity from acetate in the consortium enriched by the air-cathode MFC.

DISCUSSION

The limiting current density of *G. sulfurreducens* PCA was found to be correlated to biomass on the anode under anodic reaction-limiting conditions (Fig. 4), indicating that the per-biomass electrode reduction rate of the strain was constant as demonstrated previously (36). By using various anode surface areas, anodic (biocatalytic) reaction-limiting conditions were produced (Fig. 2). This allowed us to determine the ability of *G. sulfurreducens* PCA to transfer electrons to the carbon cloth

electrode in the MFC relative to other electron acceptors. The per-biomass electron transfer rate to the electrode was considerably lower than that obtained with fumarate or soluble iron, but it was similar to that achieved with solid iron. Theoretically, the per-biomass electron flux is influenced by the redox potential of the electron-accepting reaction (23, 28, 35) (Table 2). However, the electron flux to the anode was considerably lower than that estimated from oxygen reduction on the cathode in the air-cathode MFC. This phenomenon suggests that the electron transport system to the extracellular solid electron acceptor is the rate-limiting step for the *G. sulfurreducens* strain PCA, as it is to solid Fe(III) oxide (3, 37, 40).

Previous reports by others have shown electrode reduction rates of 47 fmol cell⁻¹ day⁻¹ to pectin-coated carbon paper (41) and rates of 870 μmol g of protein⁻¹ min⁻¹ to an unpolished graphite stick (36), both of which are much higher than those determined in the present study. Richter et al. also reported that electron transfer rates of the strain PCA to carbon cloth and flat gold were 240 μmol g of protein⁻¹ min⁻¹ and 202 μmol g of protein⁻¹ min⁻¹, respectively (37). These previous determinations, however, were based on experiments using set anode potentials in two-chambered MFCs, not in MFCs where the anode potential is determined by the physiological response of the bacterium or community. Thus, we hypothesize that these higher conversion rates of substrate into the cell mass rate resulted from the added energy input required to set the anode potential, and such results cannot be used to predict what would be achieved in an actual MFC (as examined here). Raising the anode potential allows a greater capture of energy from the respiratory chain used by bacteria, and thus, more energy can be used from the substrate for cell growth.

The maximum power densities measured here cannot be directly compared to previous results using this bottle reactor (22) due to differences in the composition of the medium and the electrode surface areas. Power production changes with anode and cathode polarizations and differences in ohmic resistances. Cathode polarization per current density normalized to anode surface area is highly affected by the anode/cathode ratio (Fig. 1B; see Fig. S3 in the supplemental material) and the reactor configuration (16, 24, 35, 39). Ohmic resistance is strongly affected by electrode spacing, membrane, and solution conductivity. For example, the previous maximum power density for a consortium was 600 mW/m² with power normalized to the cathode (4.9 cm²; a single side containing a platinum catalyst) or 130 mW/m² with power normalized to the anode (22.5 cm²; both sides of the anode), but the reactor had a fixed anode-to-cathode ratio of 4.6:1. Here, the power densities normalized to the anode ranged from 114 to 576 mW/m² for

TABLE 2. Theoretical potentials under the condition that the anode electrolyte has a pH of 7^a

Reaction	Half reaction	E', pH = 7 vs SHE
Acetate oxidation	CH ₃ COO ⁻ + 4H ₂ O → 8e ⁻ + 9H ⁺ + 2HCO ₃ ⁻	-0.296 V ^b
Fumarate reduction	(CHCOO) ₂ ²⁻ + 2H ⁺ + 2e ⁻ → (CH ₂ COO) ₂ ²⁻	+0.031 V
Ferric reduction	Fe ³⁺ + e ⁻ → Fe ²⁺	+0.771 V
Oxygen reduction	O ₂ + 4H ⁺ + 4e ⁻ → 2H ₂ O	+0.816 V

^a Calculated from Gibbs free energy using data from reference 43.

^b Calculated at typical conditions of an MFC (HCO₃⁻ = 5 mM; CH₃COO⁻ = 5 mM).

TABLE 3. Comparison of electricity-generating performance under anodic reaction-limiting conditions

Parameter	MFC	
	<i>Geobacter sulfurreducens</i> ^a	Consortium
Maximum power density (mW/m ²)		
Normalized by anode area ^b	461 ± 8	576 ± 25
Normalized by cathode area ^c	659 ± 11	1,293 ± 56
Maximum power output (W/m ³) ^d	0.87 ± 0.02	1.70 ± 0.07
Limiting current density (mA/m ²)	1,530 ± 102	1,250 ± 87
Anode biomass (μg protein/cm ²)	534 ± 43	208 ± 20
Per-biomass electrode-reducing rate (μmol g of protein ⁻¹ min ⁻¹)	178	374
Anode potential (mV vs SHE) ^e	-285	-350

^a Values were determined on day 216.

^b Anode area of *Geobacter sulfurreducens* MFC was 7 cm², and that of the consortium MFC was 11 cm².

^c Cathode areas of MFCs were 4.9 cm².

^d Volume of MFCs was 350 ml.

^e Anode potential was determined for an open circuit.

anode-to-cathode ratios of 15:1 to 2.2:1 for the MFC with the consortium (Fig. 2B). A carbonate buffer was used here, compared to a phosphate buffer in the previous tests, and both buffer composition and ionic strength are known to affect power (9, 10, 22).

It is possible to compare maximum power densities between *G. sulfurreducens* and the consortium here because the same solutions were used, and the effect of anode size was monitored in each set of experiments. As shown in Fig. 2B, the maximum power density of the consortium was consistently greater than that of the pure culture of *G. sulfurreducens* (Fig. 2B). Based on the different limiting currents and cell densities (Fig. 2A), we believe that the most useful comparison is based on per-biomass current generation and power generation under anodic reaction-limiting conditions because the limiting current densities proportionally increased with anode biomass (Fig. 4). Under anodic reaction-limiting conditions, the maximum power density was 576 ± 25 mW/m² (27.8 W/g of protein) for the consortium and 461 ± 8 mW/m² (9.0 W/g of protein) for *G. sulfurreducens* (Table 3; Fig. 5). Our result reveals a greater power density on the basis of power normalized to both anode surface area and biomass by the mixed culture than by the pure culture, which differs from results recently reported by Nevin et al. (31). They found that the power density was greater (1,900 mW/m²) using a pure culture of *G. sulfurreducens* than that obtained using a wastewater-derived consortium (1,600 mW/m²; power normalized to one side of the anode). They made this comparison using an MFC with an anode-to-cathode ratio of 1:8 and using a chemical catholyte (ferricyanide) that minimized oxygen intrusion. When *G. sulfurreducens* was examined for power production using a 1:1 (anode/cathode) ratio of electrodes in their study, the maximum power was 390 mW/m² with ferricyanide and 240 mW/m² with an air cathode. They did not report power output using smaller anodes with a mixed-culture inoculum and an air

cathode and did not investigate the microbial composition of the consortium biofilm, the biofilm densities, or the per-biomass activity. They found that placing the MFC with a ferricyanide catholyte into a glove box increased power production, presumably as a result of less oxygen leakage into the system.

We believe one of the main reasons for the greater per-biomass power density of the consortium than the pure culture shown here was that the consortium produced a more-negative anode potential than the pure culture and thus was capable of a greater working cell potential. As shown by the data in Fig. 5, the anode potential of the consortium was 65 mV lower than that of the pure culture MFC. The maximum per-biomass electrode reduction rate of the consortium was also two times higher than that of the pure culture MFC (Table 3). These two parameters define the maximum per-biomass power generation of the biofilm on the anode (Fig. 5). Because these results were obtained using otherwise identical MFC devices and solutions, these differences must be attributed to the characteristics of the biofilms. Thus, the consortium consisting primarily of *G. sulfurreducens* had a greater biocatalytic performance than a biofilm of only this pure culture. The better performance of the consortium could have been due to the efficient oxygen scavenging from the liquid solution by facultative anaerobes or the presence of bacteria that are better able to transfer electrons to the anode (reduced contact resistance). To better address the extent to which these factors are important, the molecular ecology of the anode consortium and electron transfer mechanisms from the consortium to the anode will require further study.

In summary, the present study provided a method to assess the specific electrode reduction rate of an electricity-generating microorganism or consortium from the limiting current density and anode biomass. In order to compare biocatalytic properties among anode-reducing microbes, anodic reaction-

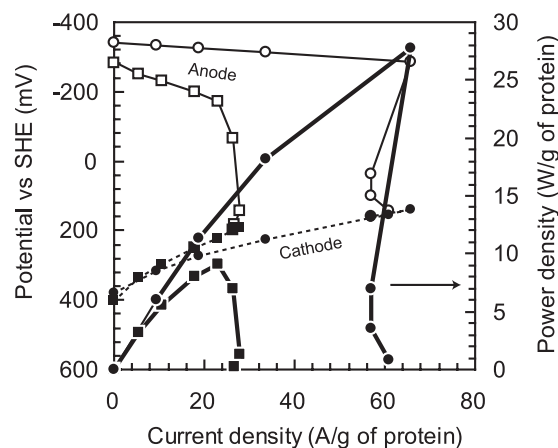


FIG. 5. Comparison of electricity-generating properties between *Geobacter sulfurreducens* cells and the enriched consortium in air-cathode MFC under anodic reaction-limiting conditions. Per-biomass power density (thick line), anode potential (thin line), and cathode potential (broken line) were plotted versus per-biomass current density. The *Geobacter sulfurreducens* cell (squares) was determined under 7 cm² of the anode surface area on day 216 (biomass density was 534 μg of protein/cm²), and the enriched consortium (circles) was determined under 11 cm² of the anode surface area on day 28 (biomass density was 208 μg of protein/cm²), respectively.

limiting conditions can be produced using an anode that is small relative to the size of the cathode. Per-biomass parameters reveal a clear comparison between electricity-generating microbes in the MFC. We are currently conducting additional tests to compare the electrode reduction rates of different species of electricity-generating microbes to find the most effective electrode reduction microbes.

ACKNOWLEDGMENTS

We thank Meng Xian Ying for technical assistance of the SEM observation and Akiko Ohashi for technical assistance of clone analysis. We also thank Yuri Gorby, Tomoyuki Kosaka, and Taku Uchiyama for valuable discussions.

This work was supported by the Japan Society for the Promotion of Science (JSPS) and the U.S. Air Force Office of Scientific Research.

REFERENCES

- Barton, S. C., J. Gallaway, and P. Atanassov. 2004. Enzymatic biofuel cells for implantable and microscale devices. *Chem. Rev.* **104**:4867–4886.
- Biffinger, J. C., J. Pietron, R. Ray, B. Little, and B. R. Ringeisen. 2007. A biofilm enhanced miniature microbial fuel cell using *Shewanella oneidensis* DSP10 and oxygen reduction cathodes. *Biosens. Bioelectron.* **22**:1672–1679.
- Bond, D. R., and D. R. Lovley. 2003. Electricity production by *Geobacter sulfurreducens* attached to electrodes. *Appl. Environ. Microbiol.* **69**:1548–1555.
- Caccavo, F., Jr., D. J. Lonergan, D. R. Lovley, M. Davis, J. F. Stolz, and M. J. McInerney. 1994. *Geobacter sulfurreducens* sp. nov., a hydrogen- and acetate-oxidizing dissimilatory metal-reducing microorganism. *Appl. Environ. Microbiol.* **60**:3752–3759.
- Chaudhuri, S. K., and D. R. Lovley. 2003. Electricity generation by direct oxidation of glucose in mediatorless microbial fuel cells. *Nat. Biotechnol.* **21**:1229–1232.
- Cheng, S., H. Liu, and B. E. Logan. 2006. Increased performance of single-chamber microbial fuel cells using an improved cathode structure. *Electrochem. Commun.* **8**:489–494.
- Cheng, S., H. Liu, and B. E. Logan. 2006. Increased power generation in a continuous flow MFC with advective flow through the porous anode and reduced electrode spacing. *Environ. Sci. Technol.* **40**:2426–2432.
- Davis, F., and S. P. Higson. 2007. Biofuel cells—recent advances and applications. *Biosens. Bioelectron.* **22**:1224–1235.
- Fan, Y., H. Hu, and H. Liu. 2007. Sustainable power generation in microbial fuel cells using bicarbonate buffer and proton transfer mechanisms. *Environ. Sci. Technol.* **41**:8154–8158.
- Feng, Y., X. Wang, B. E. Logan, and H. Lee. 2008. Brewery wastewater treatment using air-cathode microbial fuel cells. *Appl. Microbiol. Biotechnol.* **78**:873–880.
- Ishii, S., J. Koki, H. Unno, and K. Hori. 2004. Two morphological types of cell appendages on a strongly adhesive bacterium, *Acinetobacter* sp. strain Tol 5. *Appl. Environ. Microbiol.* **70**:5026–5029.
- Ishii, S., T. Kosaka, K. Hori, Y. Hotta, and K. Watanabe. 2005. Coaggregation facilitates interspecies hydrogen transfer between *Pelotomaculum thermopropionicum* and *Methanothermobacter thermoautotrophicus*. *Appl. Environ. Microbiol.* **71**:7838–7845.
- Ishii, S., T. Shimoyama, Y. Hotta, and K. Watanabe. 2008. Characterization of a filamentous biofilm community established in a cellulose-fed microbial fuel cell. *BMC Microbiol.* **8**:6.
- Kaku, N., N. Yonezawa, Y. Kodama, and K. Watanabe. 2008. Plant/microbe cooperation for electricity generation in a rice paddy field. *Appl. Microbiol. Biotechnol.* **79**:43–49.
- Karlin, S., and S. F. Altschul. 1990. Methods for assessing the statistical significance of molecular sequence features by using general scoring schemes. *Proc. Natl. Acad. Sci. USA* **87**:2264–2268.
- Kim, B. H., I. S. Chang, and G. M. Gadd. 2007. Challenges in microbial fuel cell development and operation. *Appl. Microbiol. Biotechnol.* **76**:485–494.
- Kim, J. R., S. Cheng, S. E. Oh, and B. E. Logan. 2007. Power generation using different cation, anion, and ultrafiltration membranes in microbial fuel cells. *Environ. Sci. Technol.* **41**:1004–1009.
- Lane, D. J. 1991. 16S/23S rRNA sequencing, p. 115–175. *In* E. Stackebrandt and M. Goodfellow (ed.), *Nucleic acid techniques in bacterial systematics*, John Wiley and Sons, New York, NY.
- Lin, C., and D. A. Stahl. 1995. Taxon-specific probes for the cellulolytic genus *Fibrobacter* reveal abundant and novel equine-associated populations. *Appl. Environ. Microbiol.* **61**:1348–1351.
- Liu, H., and B. E. Logan. 2004. Electricity generation using an air-cathode single chamber microbial fuel cell in the presence and absence of a proton exchange membrane. *Environ. Sci. Technol.* **38**:4040–4046.
- Liu, H., S. Cheng, and B. E. Logan. 2005. Production of electricity from acetate or butyrate using a single-chamber microbial fuel cell. *Environ. Sci. Technol.* **39**:658–662.
- Logan, B., S. Cheng, V. Watson, and G. Stadt. 2007. Graphite fiber brush anodes for increased power production in air-cathode microbial fuel cells. *Environ. Sci. Technol.* **41**:3341–3346.
- Logan, B. E., B. Hamelers, R. Rozendal, U. Schroder, J. Keller, S. Freguia, P. Aelterman, W. Verstraete, and K. Rabaey. 2006. Microbial fuel cells: methodology and technology. *Environ. Sci. Technol.* **40**:5181–5192.
- Logan, B. E., and J. M. Regan. 2006. Electricity-producing bacterial communities in microbial fuel cells. *Trends Microbiol.* **14**:512–518.
- Lovley, D. R. 2006. Microbial fuel cells: novel microbial physiologies and engineering approaches. *Curr. Opin. Biotechnol.* **17**:327–332.
- Lovley, D. R., and E. J. P. Phillips. 1986. Availability of ferric iron for microbial reduction in bottom sediments of the freshwater tidal Potomac. *Appl. Environ. Microbiol.* **52**:751–757.
- Lovley, D. R., and E. J. P. Phillips. 1986. Organic matter mineralization with the reduction of ferric iron in anaerobic sediments. *Appl. Environ. Microbiol.* **51**:683–689.
- Madigan, M. T., J. M. Martinko, and J. Parker. 2003. Anaerobic way of life, p. 576–613. *In* M. T. Madigan (ed.), *Brook biology of microorganisms*, 10th ed. Pearson Education, Inc., Upper Saddle River, NJ.
- Maidak, B. L., J. R. Cole, C. T. Parker Jr., G. M. Garrity, N. Larsen, B. Li, T. G. Lilburn, M. J. McCaughey, G. J. Olsen, R. Overbeek, S. Pramanik, T. M. Schmidt, J. M. Tiedje, and C. R. Woese. 1999. A new version of the RDP (Ribosomal Database Project). *Nucleic Acids Res.* **27**:171–173.
- Nevin, K. P., and D. R. Lovley. 2000. Lack of production of electron-shuttling compounds or solubilization of Fe(III) during reduction of insoluble Fe(III) oxide by *Geobacter metallireducens*. *Appl. Environ. Microbiol.* **66**:2248–2251.
- Nevin, K. P., H. Richter, S. F. Covalla, J. P. Johnson, T. L. Woodard, A. L. Orloff, H. Jia, M. Zhang, and D. R. Lovley. 2008. Power output and coulombic efficiencies from biofilms of *Geobacter sulfurreducens* comparable to mixed community microbial fuel cells. *Environ. Microbiol.* **10**:2505–2514.
- Oh, S., B. Min, and B. E. Logan. 2004. Cathode performance as a factor in electricity generation in microbial fuel cells. *Environ. Sci. Technol.* **38**:4900–4904.
- Park, D. H., and J. G. Zeikus. 2003. Improved fuel cell and electrode designs for producing electricity from microbial degradation. *Biotechnol. Bioeng.* **81**:348–355.
- Pham, T. H., J. K. Jang, I. S. Chang, and B. H. Kim. 2004. Improvement of cathode reaction of a mediatorless microbial fuel cell. *J. Microbiol. Biotechnol.* **14**:324–329.
- Rabaey, K., and W. Verstraete. 2005. Microbial fuel cells: novel biotechnology for energy generation. *Trends Biotechnol.* **23**:291–298.
- Reguera, G., K. P. Nevin, J. S. Nicoll, S. F. Covalla, T. L. Woodard, and D. R. Lovley. 2006. Biofilm and nanowire production leads to increased current in *Geobacter sulfurreducens* fuel cells. *Appl. Environ. Microbiol.* **72**:7345–7348.
- Richter, H., K. McCarthy, K. P. Nevin, J. P. Johnson, V. M. Rotello, and D. Lovley. 2008. Electricity generation by *Geobacter sulfurreducens* attached to gold electrodes. *Langmuir* **24**:4376–4379.
- Ringeisen, B. R., E. Henderson, P. K. Wu, J. Pietron, R. Ray, B. Little, J. C. Biffinger, and J. M. Jones-Meehan. 2006. High power density from a miniature microbial fuel cell using *Shewanella oneidensis* DSP10. *Environ. Sci. Technol.* **40**:2629–2634.
- Schröder, U. 2007. Anodic electron transfer mechanisms in microbial fuel cells and their energy efficiency. *Phys. Chem. Chem. Phys.* **9**:2619–2629.
- Shi, L., T. C. Squier, J. M. Zachara, and J. K. Fredrickson. 2007. Respiration of metal (hydr)oxides by *Shewanella* and *Geobacter*: a key role for multihaem c-type cytochromes. *Mol. Microbiol.* **65**:12–20.
- Srikanth, S., E. Marsili, M. C. Flickinger, and D. R. Bond. 2008. Electrochemical characterization of *Geobacter sulfurreducens* cells immobilized on graphite paper electrodes. *Biotechnol. Bioeng.* **99**:1065–1073.
- Tender, L. M., C. E. Reimers, H. A. Stecher III, D. E. Holmes, D. R. Bond, D. A. Lowy, K. Pilobello, S. J. Fertig, and D. R. Lovley. 2002. Harnessing microbially generated power on the seafloor. *Nat. Biotechnol.* **20**:821–825.
- Thauer, R. K., K. Jungermann, and K. Decker. 1977. Energy conservation in chemotrophic anaerobic bacteria. *Bacteriol. Rev.* **41**:100–180.
- Thompson, J. D., D. G. Higgins, and T. J. Gibson. 1994. CLUSTAL W: improving the sensitivity of progressive multiple sequence alignment through sequence weighting, position-specific gap penalties and weight matrix choice. *Nucleic Acids Res.* **22**:4673–4680.
- Tsujimura, S., M. Fujita, H. Tatsumi, K. Kano, and T. Ikeda. 2001. Bioelectrocatalysis-based dihydrogen/dioxygen fuel cell operating at physiological pH. *Phys. Chem. Chem. Phys.* **3**:1331–1335.
- Watanabe, K., Y. Kodama, and S. Harayama. 2001. Design and evaluation of PCR primers to amplify bacterial 16S ribosomal DNA fragments used for community fingerprinting. *J. Microbiol. Methods* **44**:253–262.